DELPHI 97-77 CONF 63
28 July, 1997

A study of the hadronic resonance structure in the decay $\tau \to 3\pi\nu_\tau$

Preliminary

DELPHI Collaboration

R. McNulty
CERN, CH-1211 Geneva 23, Switzerland
A. Galloni
Dept. of Physics, University of Liverpool, P.O. Box 147, Liverpool L69 3BX, UK.

Abstract

The hadronic structure of the decay of the τ lepton to three charged particles, $\tau \to 3\pi\nu_\tau$, is studied using data collected by the DELPHI detector at LEP between 1992 and 1995. The invariant mass of the 3π system, $m_{3\pi}$, is fitted using the models of Kühn and Santamaria, Isgur Morningstar and Reader, and Feindt. A comparison of the data to each model is made for both the 3π spectrum and the Dalitz projections. Below $m_{3\pi}^2 = 2.3$ GeV^2, both are in good qualitative agreement. Above $m_{3\pi}^2 = 2.3$ GeV^2, anomalous behaviour is observed, consistent with the existence of a hitherto unseen decay mode of the τ through a radial excitation of the a_1 meson.

Paper submitted to the LP'97 Conference
Hamburg, July 28 - August 1st

1 Introduction

The structure of the decay of the τ to three charged pions, $\tau \rightarrow 3\pi\nu_\tau$, has been the subject of much theoretical and experimental effort [1]. It allows the weak hadronic current to be investigated and the parity violating asymmetry parameter to be determined. In addition, the spectroscopy of intermediate energy hadronic states can be studied. An understanding of the mass spectrum is also important if this channel is to be used to measure the τ neutrino mass.

In τ decays, the 3π system is expected to have the quantum numbers $J^{PC} = 1^{++}$ and to be produced predominantly via the a_1 resonance. However, many problems still exist, both in the determination of the mass and width of the a_1 meson, and in the mechanism by which the τ decays to three pions. Experiments measuring the a_1 meson parameters from direct production in hadronic interactions obtain lower values for the mass and width than those which measure it in τ decays. Values obtained from τ data alone also vary, being dependent on the model and decay mechanism which are assumed. Section 2 briefly discusses three models which this paper considers.

LEP provides an ideal environment for the study of τ pairs, which can be detected with high efficiency and low background. The various channels into which the τ decays can be distinguished with good purity and efficiency using the DELPHI detector, which is described in section 3. Section 4 describes how a sample of precisely reconstructed events from the decay $\tau \rightarrow 3\pi\nu_\tau$ can be separated from other τ decays. Due to the excellent tracking detectors and in particular the presence of silicon microvertex detectors, the invariant mass of the three pion system can be measured with a typical precision of 20 MeV. The high purity and precise mass measurement allow various models to be compared. Section 5 describes the fits to the models while results and discussions are presented in section 6 and conclusions in section 7.

2 Theoretical Models

The models of Kühn and Santamaria [2] (KS), Isgur, Morningstar and Reader [3] (IMR) and Feindt [4] have been reasonably successful in describing the decay $\tau \rightarrow 3\pi\nu_\tau$. All assume that the decay proceeds predominantly through the a_1 resonance.

The KS model allows the τ to decay to a_1 which then decays to a mixture of $\rho\pi$ and $\rho'\pi$ which exist in the lowest dimensional Born state (approximately the S-wave state). The resonances are parameterised as Breit-Wigner functions with energy dependent widths. Constant form factors are employed in describing the $a_1 \rightarrow \rho\pi$ and $\rho \rightarrow \pi\pi$ vertices.

The IMR model allows the τ to decay to the axial-vector a_1 and the pseudo-scalar $\pi(1300)$. The a_1 decays through both D-wave and S-wave $\rho\pi$ states, as well as through the K^*K channel. The $\pi(1300)$ decays to $\rho\pi$ and a broad $\pi\pi$ S-wave state. In addition, the model makes use of a three parameter polynomial background term which was found necessary in order to "take into account many possible small effects ... e.g., the low-mass tails of radial excitations of the a_1 and ρ." The most significant difference with KS, however, is the employment of strong, energy dependent form factors. It is principally this which causes the large differences in the mass and width of the a_1 [5] as measured in τ decays.

[1] See the mini review in PDG 1996 and references therein[1].

The Feindt model is similar to the KS and IMR models but is of a more general form, allowing any combination of intermediate resonances and spin states. By appropriate selection of decay channels and form factors, it can look like KS or like IMR. Its versatility is particularly useful in evaluating the effects of different combinations of decay channels.

3 The DELPHI detector

DELPHI is well suited to this analysis, having excellent tracking components and good photon identification. The detector is described in detail elsewhere [6]. This section briefly describes the sub-detectors used in this analysis.

Charged particles are measured in the tracking chambers which are situated inside a 1.2 T super-conducting solenoid. The main tracking chamber is a time projection chamber (TPC) situated between radii of 35 cm and 120 cm. It reconstructs tracks with a typical precision in the $R\phi$ plane [2] of 300 μm, and in the Rz plane of 1 mm. Inside the TPC, between radii of 12 cm and 35 cm, is the Inner Detector (ID), a jet chamber with a typical $R\phi$ precision of 60 μm. Outside the TPC, between radii of 200 cm and 210 cm, is the Outer Detector (OD) which has an effective $R\phi$ precision of 300 μm. Close to the interaction region, lies the microvertex detector (μVD); three planes of silicon strip detectors at radii of 6.3, 9.0 and 11.0 cm. They have an $R\phi$ precision of 7 μm and a two track resolution of 100 μm.

For tracks reconstructed with all four detector elements a momentum precision of $\delta(1/p_t) = 8 \times 10^{-4}$ (GeV)$^{-1}$ is obtained, and a track extrapolation precision close to the interaction region of $23 \oplus 55p^{-1}(\sin\theta)^{-1.5}$ μm, where p is the momentum in GeV and θ is the polar angle.

Outside the tracking chambers are the electro-magnetic and hadronic calorimeters. The electro-magnetic calorimeter (HPC), situated between radii of 210 cm and 240 cm, provides measurements of both the energy and position of a shower. The energy resolution is measured to be $\delta E/E = 0.31 \times (E/\mathrm{GeV})^{-0.44} \oplus 0.027$ while the spatial precision is 1 mrad in polar angle and 2 mrad in azimuthal angle.

The hadron calorimeter is situated outside the solenoid coil and presents nine interaction lengths of iron. Outside this lie the muon chambers wherein a hit usually signifies the presence of a muon.

4 Selection of the Decay $\tau \to 3\pi\nu_\tau$

This analysis uses the data taken between 1992 and 1995, corresponding to about 4 million hadronic Z decays, or about 200,000 τ pairs. The selection of $\tau \to 3\pi\nu_\tau$ candidates starts by identifying decays of the Z to two τ leptons produced back to back, one of which decays to three charged particles, while the other decays to one or three charged particles. Two hemispheres are defined perpendicular to the thrust axis, and it is required that one hemisphere contains three tracks which are each isolated by at least 160° from all tracks in the other hemisphere. The following conditions are then placed on the three tracks in order to reduce backgrounds. The vector sum of their momenta must exceed 10 GeV. The

[2] R, ϕ and z define a polar co-ordinate system with the origin at the interaction point and the z axis along the electron direction.

total electro-magnetic energy in a cone of 15° about the vector sum of the three tracks must be less than half their summed momenta. The typical signature of a π^0 in DELPHI is either two neutral electro-magnetic clusters, or one high energy neutral deposit. Thus to reject $\tau \rightarrow \pi\pi\pi(n\pi^0)\nu_\tau$ decays, events having two or more neutral energy deposits greater than 500 MeV or events with a single deposit greater than 2 GeV are rejected. The event is also removed if any of the three tracks points to hits in the muon chambers and has deposits in the hadron calorimeter consistent with a minimum ionising particle. It is possible that such events originate from four-fermion processes.

The track reconstruction algorithm follows closely that used in the DELPHI determination of the τ lifetime [7], with tight requirements on both track and vertex reconstruction quality. Starting from the TPC track elements, extrapolations are made inwards to the μVD, where all possible hit combinations are considered. ID and OD elements are added to the candidate tracks where possible. All three tracks are required to have at least two hits in the μVD. A vertex fit is performed in the transverse plane, for every combination of candidate tracks. It is required that a unique combination of track elements exists which have a track fit and vertex fit probability greater than 1%. This cut is chosen as the distributions are flat above this value, and rise sharply below it due to random combinations. The reconstructed vertex is required to lie within 3 cm of the beam-spot in order to reject photon conversions in the beam-pipe.

The invariant mass squared s of the system is calculated at the vertex assuming the pion mass for all three particles. The resolution on $\sqrt{s}$ is typically between 10 and 35 MeV with an average of 22 MeV for a mass of 1.2 GeV, and between 15 and 55 MeV with an average of 36 MeV for a mass of 1.6 GeV. The invariant mass squared of pairs of oppositely charged particles is found assuming the pion mass. A total of 7180 events remain after all cuts.

The selection requirements for identifying the decay $\tau \rightarrow 3\pi\nu_\tau$ have been made considering the various background processes, both from other τ decays involving kaons or unidentified π^0s and from non τ sources. These contributions were estimated using Monte Carlo simulations. The KORALZ generator [8] was used to produce τ decays which were passed through a full detector simulation. Each channels was re-weighed to the world-average value [1], except for the kaon channels where recent DELPHI results were used [19]. The $3\pi\pi^0$ channel was modified by the inclusion of the process $\tau \rightarrow \rho\pi\pi\nu$ where the pions have opposite charge. Contamination from non τ sources comes from hadronic decays of the Z and from four-fermion events. Both have been estimated from simulation. The hadronic Z decays have been generated using the LUND Parton Shower model [9], and the four-fermion events using the BDK generator [10]. An efficiency inside $|\cos\theta| < 0.73$ of 36% is obtained with a background of 20%, whose composition is detailed in Table 1. Note however that the background is not flat in s; at high values, the sample is essentially pure.

5 Comparisons with KS and IMR models

The distribution of the invariant mass squared of the three pions is fitted to the models of KS and IMR, and the a_1 parameters extracted. The Dalitz plots are compared to the predictions of both models. Anomalous behaviour in the high s region leads to some discussion of possible causes.

Channel	All s	s ranges (GeV^2)					
		$[0.8, 1.1]$	$[1.1, 1.4]$	$[1.4, 1.7]$	$[1.7, 2.0]$	$[2.0, 2.3]$	$[3.3, 3.5]$
$\tau \to 3\pi\nu$	5628.1 ± 36.2	1175.4	1850.2	1331.8	683.4	291.8	141.3
$\tau \to 3\pi\pi^0\nu$	1060.2 ± 16.3	306.6	255.5	146.3	54.7	13.2	1.7
$\tau \to 3\pi 2\pi^0\nu$	33.6 ± 3.0	11.3	4.4	1.4	0.0	0.0	0.0
$\tau \to K2\pi\nu$	287.8 ± 8.5	39.7	89.7	103.7	37.2	3.2	0.7
$\tau \to 2K\pi\nu$	73.6 ± 4.6	30.7	17.5	7.9	3.6	0.0	0.0
$\tau \to other$	50.6 ± 3.1	11.6	6.1	5.0	1.4	1.7	1.1
Z$\to q\bar{q}$	40.3 ± 6.3	3.9	1.3	2.6	3.9	2.6	5.2
Z$\to llll$	5.8 ± 1.2	0.0	0.0	0.0	0.0	0.0	0.4

Table 1: Estimated Sample Composition over the full s range, and in various subranges.

5.1 Fits to the invariant mass squared distribution

The distribution of the invariant mass squared s of the three pions is fitted to the models by maximising the likelihood function L, which is the product of event probabilities over the number of events N:

$$L = \prod_{i=1}^{N} \{(1-\lambda)\epsilon(s_i)P_{sig}(s_i, \sigma_i) + \lambda P_{bkg}(s_i)\}, \tag{1}$$

where P_{sig}, P_{bkg} are probability distributions describing the signal and background shapes, ϵ is the detection efficiency and λ is the proportion of background events in the sample. The signal shape is obtained by convoluting the relevant theoretical distribution with the resolution σ on an event by event basis. The simulation studies show the resolution function to be well parameterised by three Gaussian functions of widths σ, 3σ and 7σ and weights 0.950, 0.045 and 0.005 respectively. The background is taken from the generators described above combined with the detector simulation.

Results for the following models are presented:

- KS model, the parameters and masses as given in the first row of Table 1 of [2] are used. The mass and width of the a_1 meson are left as free parameters.
- IMR model, the prescription for their 'preferred' fit is followed but does not include the KK^* contributions as these do not contain 3π in the final state. [3] The PDG values [1] are taken for all masses and widths. The strong decay on-shell form factors are taken from the model predictions detailed in Appendix B of [3]. The mass of the a_1 meson is left as a free parameter as well as the three terms which characterise the polynomial background. The a_1 width is calculated from the mass in accordance with the model.

The fits are shown in Fig 1a)&b) and the a_1 parameters are given in the first two columns of Table 2. The data are in reasonably good agreement with the KS model. A

[3]The effect of the KK^* channel , where the final state kaons are mis-identified as pions, is considered when estimating the backgrounds.

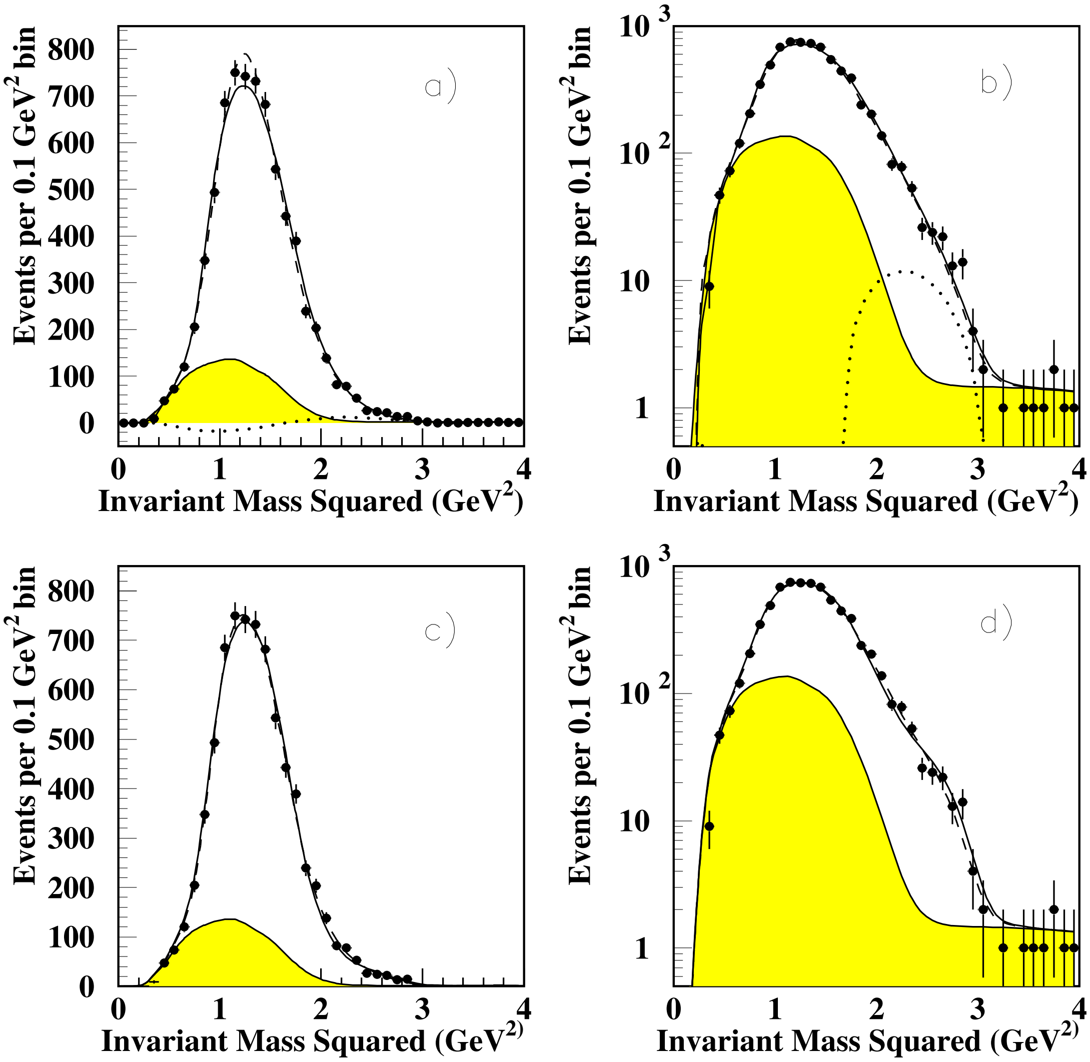

Figure 1: Distribution of 3π invariant mass squared with various models superimposed. The points are the data values. In plot a) the dashed curve is the fit to KS; the solid curve is the fit to IMR; the dotted curve indicates the contribution of the polynomial background. Plot b) is as for a) but on a log scale. In plot c) the dashed curve is the fit described as MF1-KS in the text; the solid curve is that described as MF2-IMR. Plot d) is as for c) but on a log scale.

	KS	IMR	MF1-KS	MF2-IMR
Mass (MeV)	$1249 \pm 7 \pm 9$	$1215 \pm 5 \pm 5$	$1166 \pm 4 \pm 8$	$1215 \pm 5 \pm 9$
Width (MeV)	$538 \pm 24 \pm 29$	$474 \pm 3 \pm 15$	$376 \pm 15 \pm 11$	$380 \pm 14 \pm 11$
a' amplitude (%)	-	-	$2.4 \pm 0.5 \pm 0.4$	$2.2 \pm 0.4 \pm 0.5$
χ^2/ #bins	28.8 /28	46.9/28	25.2/28	40.9/28

Table 2: Fitted a_1 parameters. The first error is statistical; the second is due to systematics.

feeling for the goodness of fit can be obtained by noting that the χ^2 over the 28 bins from $s = 0.5$ GeV^2 to $s = 3.2$ GeV^2 is 28.8. [4] Close to the endpoint, however, the data lie somewhat higher than the model predicts. The mass and width of the a_1 are measured to be 1249 ± 7 MeV and 538 ± 24 MeV respectively, which agree with previous experimental determinations [12, 13]. It is noteworthy, however, that these results predict a branching ratio $BR(\tau \to 3\pi\nu_\tau) = 7.2 \pm 0.3\%$, in disagreement with the direct measurement of this quantity [1].

The IMR model is also in reasonable agreement with the data. The χ^2 over the 28 bins from $s = 0.5$ GeV^2 to $s = 3.2$ GeV^2 is 46.9. The polynomial term contributes 3%, by area,of the total prediction. However above $s = 2.5$ GeV^2, one third of the theoretical prediction is given by the polynomial background. This could be taken as a qualitative indication of the existence of some higher mass resonance. Without the polynomial background, the fit is poor, the fitted mass rises by 8 MeV and the $\chi^2 = 74.4$.

The mass of the a_1 is measured to be 1215 ± 5 MeV and the width is calculated to be 474 ± 3 MeV. This is in agreement with previous experimental determinations, noting that the small statistical error on the width is due to holding the form factors fixed at their theoretical values whereas other experiments have chosen to fit for them.

A number of systematics which affect the determination of the a_1 parameters have been considered. The modelling of the background from other τ decays was investigated. In the $3\pi\pi^0$ channel, the mass and width of the ρ' were varied from their default values of 1.45 GeV and 0.30 GeV respectively, to a mass of 1.70 GeV and a width of 0.26 GeV, and also to a mass of 1.25 GeV and a width of 0.13 GeV. Furthermore, the channel $\tau \to \rho\pi\pi\nu$, which had been added to the KORALZ defaults, was removed. In addition the overall normalisation was changed by 10%. The normalisation of the kaon channels was varied by 30%. Systematic errors from these sources of 7 and 5 MeV for the mass, and 22 and 2 MeV for the width, were found for the KS and IMR models respectively.

The detector resolution was verified by reconstructing the D^0 mass peak from a data sample of D^* mesons which decay via $D^* \to D^0\pi \to K\pi\pi$. The mass and momentum of the D^0 are similar to those of the τ. The mass peak was fitted using the nominal 3-Gaussian resolution function described above, together with a scale factor k_1 to multiply the calculated σ and a second factor k_2 to multiply the proportion of the second Gaussian. The values obtained are $k_1 = 1.04 \pm 0.04, k_2 = 1.7 \pm 0.5$. These were used to calculate

[4] This is not a true χ^2 as it has been calculated after the fit results which used a maximum likelihood method. Bins with small numbers of events have been converted to an equivalent χ^2 using Poisson probabilities.

a systematic uncertainty. Errors from these sources of 5 and 4 MeV for the mass, and 19 and 2 MeV for the width were found for KS and IMR respectively. An additional systematic of 15 MeV is included on the a_1 width in the IMR model, due to the variations in the form factors (as given in [3]) which come from varying the string-breaking constant γ_0 from its nominal value of 0.39 [11] within its rounding error of 0.005.

5.2 The Dalitz plots and projections

Holding the parameters fixed at the values given by the relevant fits, the Dalitz plots in various s ranges are shown in the first three columns of Fig. 2 for data, KS, and the resonant part of IMR (since the shape the polynomial background would assume is unknown). The quantities s_1 and s_2 are the invariant mass squared values for the two unlike-signed particle combinations, with $s_1 > s_2$. The distributions for the models have been corrected for resolution and efficiency effects, but do not allow for the effects of non $\tau \to 3\pi$ backgrounds. In the two lower s ranges displayed, the structures apparent in the data are reproduced by the models. In the two higher s bins however, the prominent ρ bands of the KS model are not reproduced in the data. The resonant part of the IMR model provides better agreement [5], although the normalisation (which is not apparent in the Dalitz plots) is very different.

To better judge the agreement between the data and the models, the Dalitz plots are projected onto their axes (Fig. 3). The normalisation is now clear and the background contributions that the simulations predict have been included. To evaluate the goodness of fit, the chi-squared and number of degrees of freedom are given in the first two columns of Table 3.

Below $s = 2.3$ GeV^2, it can be seen from Figs. 2 and 3 that both models give good qualitative agreement. They reproduce a ρ peak in about the correct position and show that the dominant decay mode proceeds via $\tau \to a_1\nu_\tau \to \rho\pi\nu_\tau \to \pi\pi\pi\nu_\tau$. As pointed out previously by OPAL [12] and ARGUS [13], there is some evidence of minor discrepancies between the data and the model predictions. It is possible that relatively small modifications to the models could explain these discrepancies, for example IMR describe possible mass shift functions and KS enter into some discussion on the parameterisation of the Breit-Wigners.

Above $s = 2.3$ GeV^2, where an excess of events is observed in the s distribution, the first Dalitz projection in Fig. 3 shows an excess of events at $\sqrt{s_1}$ of about 1.25 GeV, in disagreement with the models.

5.3 Discussion

Taking into account phase space effects, the enhancement observed at $\sqrt{s_1}$ of about 1.25 GeV for s above 2.3 GeV^2 could be explained by a decay channel of the τ through a wide resonance of mass similar to or greater than the τ mass which then decays to 3π via the intermediate state of a pion plus a particle of mass 1.25 GeV or greater.

An excellent candidate for such a decay is the a_1', which is a radial excitation of the a_1 meson. It is predicted in the flux-tube breaking model of Isgur and Kokoski [11] to have

[5] The double peaked shape of the Dalitz plots for IMR at high s is due to the energy dependent form factors which create the $\rho\pi$ predominantly in the D-wave state here. KS assumes an S-wave state at all energies.

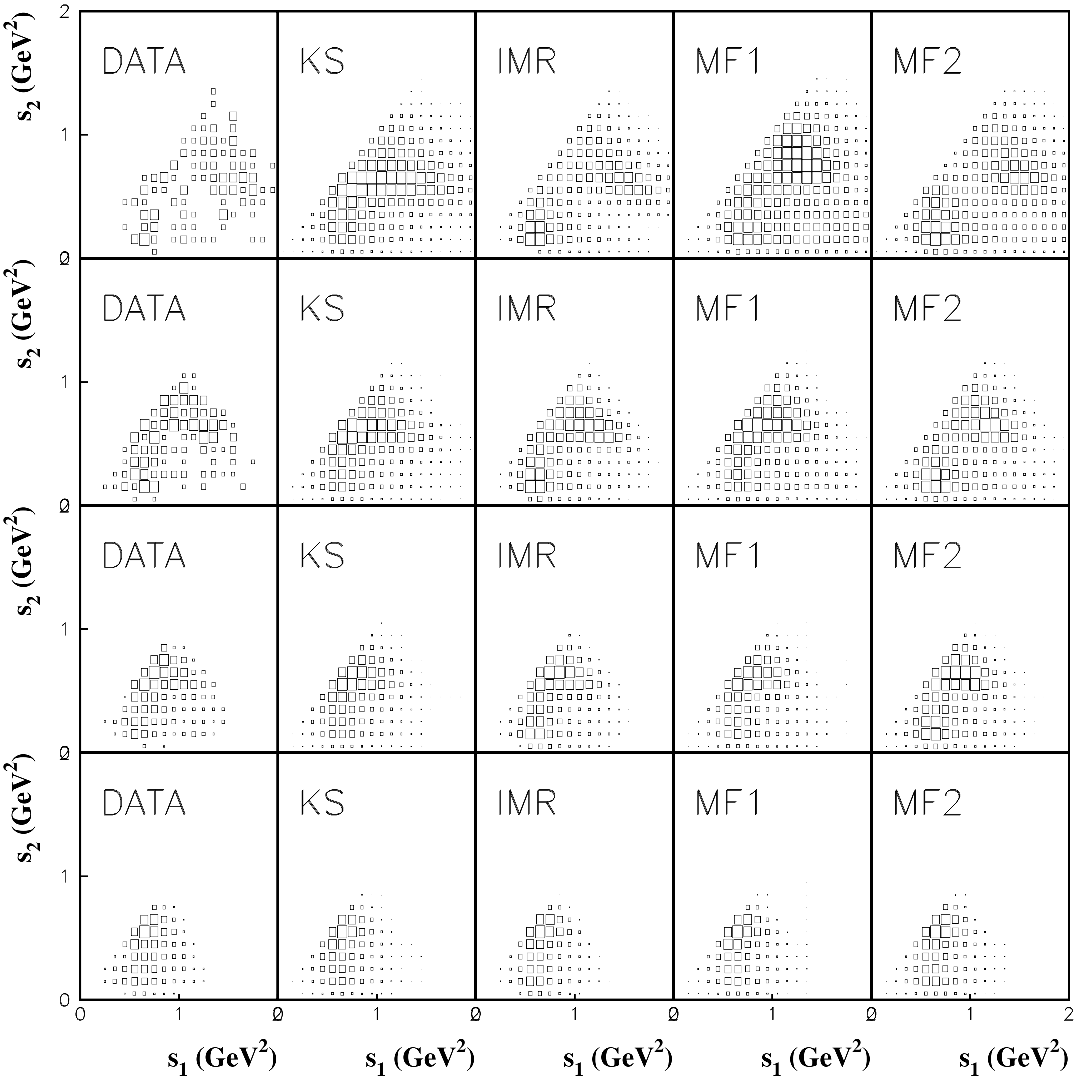

Figure 2: Dalitz plots in sequential s ranges, for the data and the models described in the text. From top to bottom the s ranges (in units of GeV^2) are: $2.3 < s < 3.5$; $2.0 < s < 2.3$; $1.7 < s < 2.0$; $1.4 < s < 1.7$.

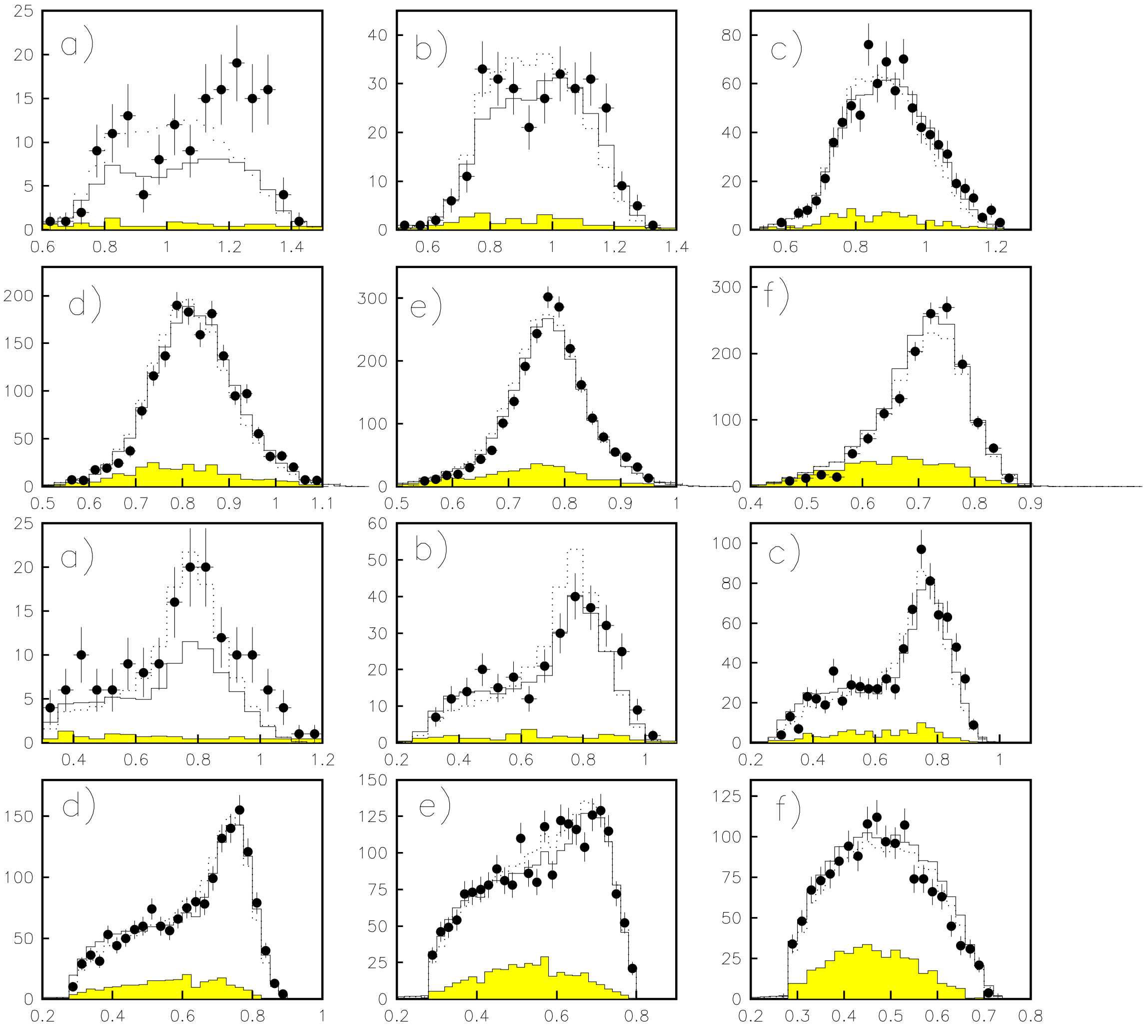

Figure 3: Distributions for $\sqrt{s}_1$ and $\sqrt{s}_2$ for various s bins. The top six plots are for $\sqrt{s_1}$; the bottom six are for $\sqrt{s_2}$. The six s regions (in units of GeV^2) are: a) $2.3 < s < 3.2$; b) $2.0 < s < 2.3$; c) $1.7 < s < 2.0$; d) $1.4 < s < 1.7$; e) $1.1 < s < 1.4$; f) $0.8 < s < 1.1$. The points represent the data; the dotted line is the KS fit; the solid line is the resonant part of the IMR fit; the shaded histogram is the background. Units on the horizontal axis are in GeV^2.

Range	KS χ^2 / ndf	IMR χ^2 / ndf	MF1-KS χ^2 / ndf	MF2-IMR χ^2 / ndf
s_1 (GeV^2)				
$2.3 < s < 3.5$	55.9 / 18	86.9 / 18	32.0 / 18	18.5 / 18
$2.0 < s < 2.3$	27.6 / 18	26.6 / 18	26.7 / 18	24.5 / 18
$1.7 < s < 2.0$	64.0 / 32	62.0 / 32	74.3 / 32	61.2 / 32
$1.4 < s < 1.7$	56.2 / 28	68.5 / 28	70.2 / 28	41.3 / 28
$1.1 < s < 1.4$	68.1 / 30	77.6 / 30	92.9 / 30	59.5 / 30
$0.8 < s < 1.1$	65.7 / 25	34.0 / 25	69.9 / 25	60.3 / 25
s_2 (GeV^2)				
$2.3 < s < 3.5$	48.8 / 18	79.0 / 18	13.2 / 18	15.0 / 18
$2.0 < s < 2.3$	42.3 / 18	27.2 / 18	13.5 / 18	27.0 / 18
$1.7 < s < 2.0$	84.1 / 32	62.1 / 32	71.5 / 32	88.0 / 32
$1.4 < s < 1.7$	34.4 / 28	41.2 / 28	33.0 / 28	31.6 / 28
$1.1 < s < 1.4$	41.5 / 30	48.9 / 30	38.7 / 30	40.0 / 30
$0.8 < s < 1.1$	39.7 / 30	35.1 / 30	40.2 / 30	41.6 / 30

Table 3: χ^2 and the number of degrees of freedom for the agreement between data and the various model predictions.

a mass of 1820 MeV and to decay to the $\rho\pi$ D-wave state in preference to the S-wave state. Such a resonance has probably already been seen by the VES collaboration [14], which reported a clear signal in the D-wave state (and an enhancement of equal size in the S-wave), for a $J^{PC} = 1^{++}$ particle with a mass of about 1700 MeV and a width of about 300 MeV. If this exists, then there is every reason to expect it to be present in τ decays, and in fact Iizuka et al. [15] have already postulated such a particle as a means of reconciling the discrepancy in the a_1 parameters measured in hadronic experiments and in τ decays. Furthermore, Shuryak and Kapusta [16] use Weinberg sum rules to relate the vector and axial-vector τ decay modes and conclude that there is a missing contribution in the axial-vector mode which could be explained by an a_1'.

VES also reported a similar signal in the 1^{++} wave in the $f_1\pi$ channel [17]. If this is the same resonance, one might expect an enhanced production of $f_1\pi$ in τ decays. This is exactly what CLEO reported recently [18], with the first observation of the decay $\tau \to f_1\pi\nu$, at a level in excess of theoretical prediction. If it is assumed that the same resonance is responsible for the VES, CLEO and DELPHI signals then, from CLEO's reported branching ratio and the relative probabilities which VES observe for the decays of this resonance to $f_1\pi$, $(3\pi)_S$ and $(3\pi)_D$, a branching ratio for $\tau \to a'\nu \to 3\pi\nu$ of order 10^{-3} can be predicted.

6 Studies with the Feindt model

Two fits to the s distribution are made using the Feindt model. In the first (MF1-KS), it is assumed that the a_1 decays as in the KS prescription but, in addition, the τ is allowed to decay through an a_1'. In the second (MF2-IMR), it is assumed that the a_1 decays as in the IMR prescription using the strong form factors and D/S wave ratio predicted by this model. However, instead of employing a polynomial background term, the τ is also allowed to decay through an a_1'. The a_1' is described by a Breit-Wigner function with a mass of 1700 MeV and a width of 300 MeV, and is allowed to decay with equal probability into the S-wave $\rho'\pi$ state and the D-wave $\rho\pi$ state, as suggested by the VES results.

The results of the fits are given in the last two columns of Table 2. Note that the fitted mass and width of the a_1 for MF1-KS are very different from those for KS and are close to the values obtained in hadronic production experiments. Since the only difference between MF1-KS and KS is the addition (of a small amount $\approx 2.3\%$) of a_1', it is observed that the a_1 width is very sensitive to the addition of higher mass resonances in the 3π spectrum. This might help explain the discrepancy between the parameters of the a_1 measured in τ decay and in hadronic production.

The fit to the s distribution is shown in Fig. 1c)&d). The χ^2 over the 28 bins from $s = 0.5$ GeV^2 to $s = 3.2$ GeV^2 is 25.2 for MF1-KS, which is better than for KS; for MF2-IMR, $\chi^2 = 40.9$ which is better than for IMR. This improvement occurs principally in the high s region.

The Dalitz plots are shown in the last two columns of Fig. 2. MF2-IMR shows she same characteristics in the high s plots as the data. The agreement of MF1-KS is less striking, but better than KS. The projections are shown in Fig. 4, while the goodness of fit in each of the histograms is given in the last two columns of Table 3. The improvement in the high s bins is marked while in the lower s bins it is roughly equivalent to the original fits.

Taking the percentage of a' to be 2.3$\pm$0.6% (table 2), and multiplying by the branching ratio for $\tau \to 3\pi\nu$, [6] the branching ratio is calculated to be

$$BR(\tau \to a'\nu \to 3\pi\nu) = (2.0 \pm 0.6) \cdot 10^{-3}.$$

This is in agreement with the tentative prediction obtained above. This agreement should not be taken as proof of this hypothesis, as many assumptions are implicit in the reasoning. Nonetheless, it provides a useful consistency check.

Other solutions should also be borne in mind. Moderate success, not reported above, has also been obtained in explaining the discrepancy using a different set of results from the VES collaboration [20], who reported the observation of a $J^{PC} = 0^{-+}$ state with an unusually small width, the $\pi(1800)$, which can decay to 3π. Unfortunately, not enough data are available to unambiguously identify the underlying cause.

7 Conclusions

The hadronic structure of the decay $\tau \to 3\pi\nu$ has been investigated.

Below $s = 2.3$ GeV^2, the 3π invariant mass distribution s is found to be in reasonable agreement with the KS and IMR models. The Dalitz plots and projections are in broad agreement with the models, showing that the decay proceeds predominantly through a_1 and ρ resonances, although close comparison shows some small discrepancies.

Above $s = 2.3$ GeV^2, an enhancement is observed, which is particularly clear in the Dalitz plots and projections. This effect is not described by the models and leads us to

[6] This has been calculated by subtracting the kaon channels [19] from the branching ratio for $\tau \to 3h\nu$ [1].

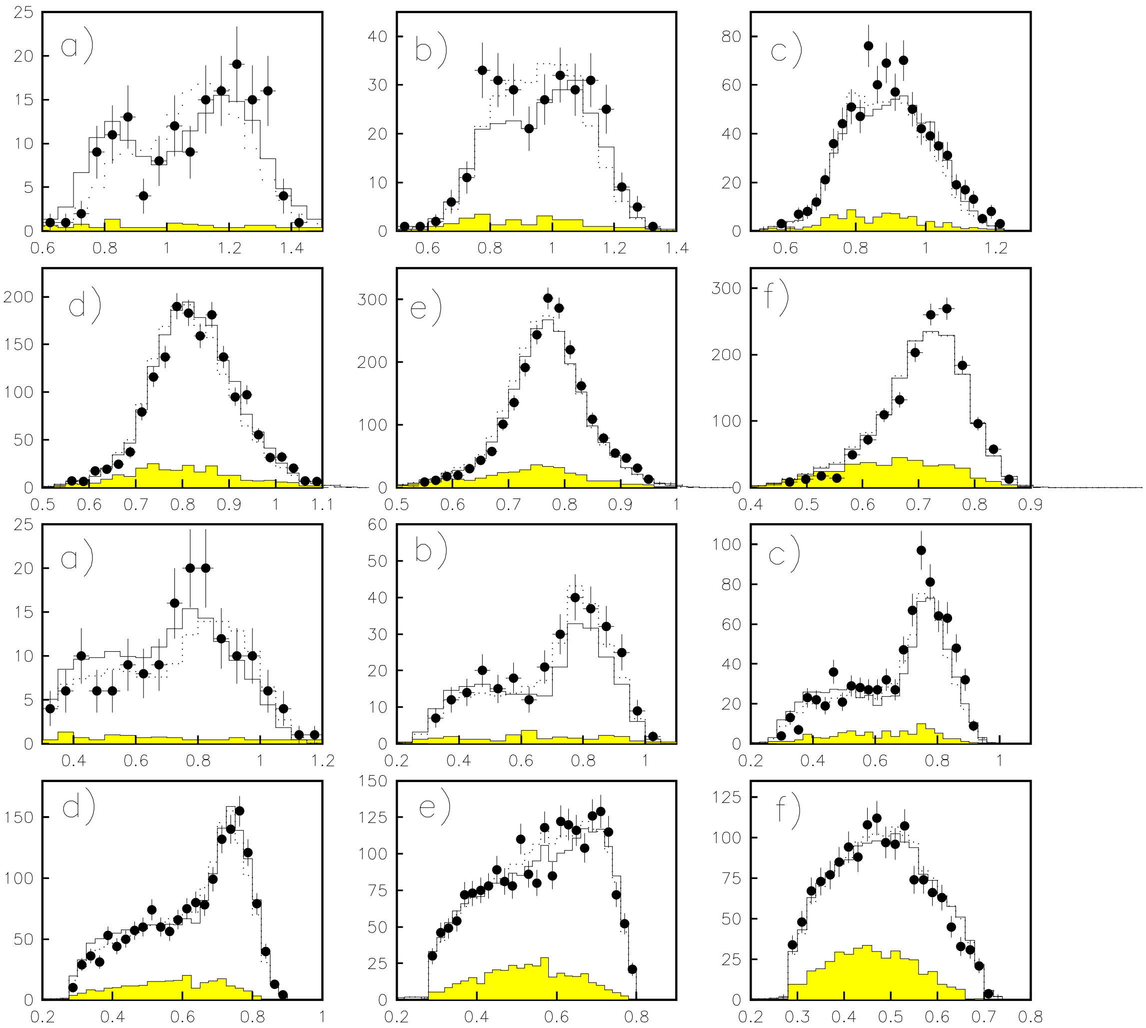

Figure 4: Distributions for $\sqrt{s_1}$ and $\sqrt{s_2}$ for various s bins. The top six plots are for $\sqrt{s_1}$; the bottom six are for $\sqrt{s_2}$. The six s regions (in units of GeV^2) are: a) $2.3 < s < 3.2$; b) $2.0 < s < 2.3$; c) $1.7 < s < 2.0$; d) $1.4 < s < 1.7$; e) $1.1 < s < 1.4$; f) $0.8 < s < 1.1$. The points represent the data; the dotted line is the fit labelled MF1-KS in the text; the solid line is the fit labelled MF2-IMR; the shaded histogram is the background from other decay processes. Units on the horizontal axis are in GeV^2.

hypothesise the existence of a hitherto unobserved decay channel in τ decays consistent with the decay chain $\tau \to a_1' \nu_\tau$.

The KS model, although providing a reasonable description of the shape of the s distribution, has three problems. Firstly, the large fitted width of the a_1 leads to a branching ratio prediction at variance with the experimentally measured value. Secondly, it does not describe an excess of events which is seen at high s values. Thirdly, the Dalitz distribution at high s differs from the data. One should therefore be cautious of using this to make measurements which depend strongly on describing the high s region correctly (eg. neutrino mass determinations).

The IMR model gives a fair description of the data, although in the high s region this is in large part due to the polynomial background term. This is clearly a weak point of the model, as it does not provide a physical explanation for the behaviour.

A better description of the data is obtained using the Feindt model to extend the models of KS and IMR by including the effect of the a'. However, this is not the only possible explanation. Unfortunately, not enough data are available to unambiguously identify the resonances which may exist in this region. Further theoretical and experimental work is required.

The observation of this effect is interesting for intermediate energy quark spectroscopy, and may help resolve some of the problems concerning the a_1 meson. It is also important in measuring the spectral functions for τ decay. A good understanding of these is necessary in order to measure the τ neutrino mass. An extra resonance close to the τ mass will distort the population of phase space close to the kinematic limit and, if not correctly accounted for, lead to erroneous results in the neutrino mass determination.

Acknowledgements

We are greatly indebted to our technical collaborators and to the funding agencies for their support in building and operating the DELPHI detector, and to the members of the CERN-SL Division for the excellent performance of the LEP collider.

References

[1] PDG96: R.M. Barnett et al., *Phys. Rev.* D**54** (1996) 345.

[2] J. H. Kühn and A. Santamaria, *Z. Phys.* C**48** (1990) 445.

[3] N. Isgur, C. Morningstar and C. Reader, *Phys. Rev.* D**39** (1989) 1357.

[4] M. Feindt, *Z. Phys.* C**48** (1990) 681.

[5] P.R. Poffenberger, *Z. Phys.* C**71** (1996) 579.

[6] P. Aarnio et al., DELPHI coll., *Nucl. Instrum. Methods* A**303** (1991) 233;
P. Abreu et al., DELPHI coll., *Nucl. Instrum. Methods* A**378** (1996) 57.

[7] P. Abreu et al., DELPHI coll., *Phys. Lett.* B**365** (1996) 448.

[8] S. Jadach, J. H. Kühn and Z. Was, Comp. Phys. Comm. **79** (1994) 503.

[9] T. Sjostrand, Comp. Phys. Comm. **82** (1994) 74.

[10] F. A. Berends, P. H. Daverveldt, R. Kleiss, Comp. Phys. Comm. **40** (1986) 271.

[11] R. Kokoski and N. Isgur, *Phys. Rev.* D**35** (1987) 907.

[12] R. Akers et al., OPAL coll., *Z. Phys.* C**67** (1995) 45;
K. Ackerstaff et al., OPAL coll., CERN-PPE/97-20.

[13] H. Albrecht et al., ARGUS coll., *Z. Phys.* C**58** (1993) 61.

[14] D. V. Amelin et al., VES Collaboration, *Phys. Lett.* B**356** (1995) 595.

[15] J. Iizuka, H. Koibuchi and F. Masuda, *Phys. Rev.* D**39** (1989) 3357.

[16] J. I. Kapusta and E. V. Shuryak, *Phys. Rev.* D**49** (1994) 4694.

[17] Yu. P. Gouz et al., *Proc. of the XXVI Int. Conf. on High Energy Physics,* Dallas, (1992) 572;
J. H. Lee et al., *Phys. Lett.* B**323** (1994) 227.

[18] V. G. Shelkov, *Proc. of TAU96*, Colorado.

[19] DELPHI contributed paper pa07-009 to ICHEP'96, Warsaw.

[20] A. M. Zaitsev, *Yadernaya Fizika* **59** (1996) 1674;
E. B. Berdnikov et al., *Yadernaya Fizika* **57** (1994) 1610.